HHS Public Access

Author manuscript

J Leukoc Biol. Author manuscript; available in PMC 2020 February 01.

Published in final edited form as:

J Leukoc Biol. 2020 February ; 107(2): 175–183. doi:10.1002/JLB.1HI0219-073RR.

Frontline Science: A flexible kink in the transmembrane domain impairs β2 integrin extension and cell arrest from rolling

Hao Sun[1], **Zhichao Fan**[2,3], **Alexandre R. Gingras**[1], **Miguel A. Lopez-Ramirez**[1], **Mark H. Ginsberg**[1], **Klaus Ley**[2,4]

[1]Department of Medicine, University of California, San Diego, La Jolla, California, USA

[2]Division of Inflammation Biology, La Jolla Institute for Immunology, La Jolla, California, USA

[3]Department of Immunology, University of Connecticut Health Center, Farmington, Connecticut, USA

[4]Department of Bioengineering, University of California, San Diego, La Jolla, California, USA

Abstract

β2 integrins are the main adhesion molecules in neutrophils and other leukocytes and are rapidly activated by inside-out signaling, which results in conformational changes that are transmitted through the transmembrane domain (TMD). Here, we investigated the biologic effect of introducing a proline mutation in the β2 integrin TMD to create a flexible kink that uncouples the topology of the inner half of the TMD from the outer half and impairs integrin activation. The β2 integrin alpha chains, αL, αM, αX, and αD, all contain an inserted (I) domain with homology to von Willebrand factor A domain. β2 activation was monitored in a homogenous binding assay of 2 reporter monoclonal antibodies: KIM127 reporting extension (E^+) and mAb24 reporting the high-affinity (H^+) conformation of the β2 I-like domain. The proline mutation partially diminished chemokine-induced extension, but not the high-affinity conformation. The proline mutation in the TMD of β2 completely inhibited arrest of rolling HL-60 cells in response to the chemokine IL-8. TMD mutant HL-60 cells rolling on P-selectin and ICAM-1 were unable to reduce their rolling velocity in response to IL-8. Quantitative dynamic footprinting live-cell imaging showed that blocking TMD topology transmission impaired the chemokine-induced activation of β2, limiting the appearance of extended high-affinity (E^+H^+) β2. This also resulted in a defect in early spreading (3 min after arrest), which could be overcome by forced integrin activation using Mn^{2+}. We conclude that the TMD proline mutation severely impairs β2 integrin extension, cell arrest, and early spreading.

Correspondence Klaus Ley, Division of Inflammation Biology, La Jolla Institute for Immunology, La Jolla 92037, CA, USA. klaus@lji.org.

AUTHORSHIP

H.S., Z.F., and K.L. conceived the project and designed experiments. H.S. and Z.F. performed the experiments and analyzed data. M.H.G. provided key reagents and devices and contributed expert advice to the design of experiments. H.S. and K.L. wrote the manuscript with contributions from all authors. A.G. contributed the structures in figure 1A. M.A. L.-R. provided critical reagents for figure 1C. H.S. and Z.F. contributed equally.

DISCLOSURES

The authors declare no conflicts of interest.

Keywords

talin; activation; affinity; adhesion; spreading

1 | INTRODUCTION

Neutrophils and other leukocytes must arrest from rolling in order to reach sites of inflammation.[1–4] The arrest of neutrophils is triggered when β2 integrins become activated through inside-out signaling mechanisms, which are initiated by chemokines binding their G protein-coupled receptors and by P-selectin glycoprotein ligand-1 (PSGL-1) binding to endothelial E- or P-selectin.[4–7] In neutrophils, the PSGL-1 pathway of integrin activation proceeds through L-selectin, Src kinases, the spleen tyrosine kinase (Syk), and other downstream signaling intermediates, leading to β2 integrin extension, but not the high-affinity conformation.[8] E-selectin recognition of sLe^x on L-selectin also plays an important role in transitioning neutrophils from rolling to arrest.[9] The chemokine receptor pathway starts with dissociation of the Gα from the Gβγ subunits, which trigger other signaling intermediates, leading to high-affinity β2 integrin.[2] The extension (E) and the high-affinity (H) conformation of human β2 integrins can be assessed by 2 monoclonal antibodies (mAbs) that report these conformations. KIM127 binds an epitope in the knee of β2 that becomes accessible upon integrin extension[10] and mAb24 reports the high-affinity conformation of the β2 I-like domain.[11] The 2 epitopes are nonoverlapping, KIM127 and mAb24 do not cross-block each other, and neither competes with ligand binding.[3] Thus, $KIM127^+mAb24^+$ β2 integrin molecules are extended and high affinity (E^+H^+).[3,12] The E^+H^+ conformation is the only conformation that can mediate arrest from rolling. $KIM127^+$ $mAb24^-$ (E^+H^-) β2 integrins mediate transient binding, which results in slow rolling.[3,8] $KIM127^-$ $mAb24^+$ integrins (E^-H^+) are high affinity but remain bent and thus bind ligands like ICAM-1 in cis (on the same cell)[3,12] and do not participate in arrest. Instead, E^-H^+ integrins strongly reduce neutrophil adhesion.

The β2 integrin cytoplasmic tail can bind talin-1 and kindlin-3.[13] Cells without talin-1 cannot activate integrins at all (integrins remain E^-H^-), whereas cells without kindlin-3 cannot induce the high-affinity conformation, but can still extend (E^+H^-) and produce slow rolling.[14] When talin binds β2, a conformational change is induced that results in a change of the angle of the β2 transmembrane domain (TMD) relative to the plasma membrane.[15,16] Because the transmembrane α helix is relatively stiff, this angle change is transmitted to the extracellular domain and results in extension.[17,18] Introducing a mutation in the ninth amino acid from the C terminus of the TMD prevents the transmission of the conformational change in β7 integrins[19] and β3 integrins.[20]

Here, we tested how a similar mutation (L697P) in β2 alters integrin activation and attendant cell function. Unlike β3 and β7, the α chains pairing with β2, αL, αM, αX, and αD, all contain an inserted (I) domain, also known as A domain with homology to von Willebrand factor. Using the conformation-reporting mAbs KIM127 and mAb24 for human β2, we can assess the exact effect of the L697P mutation on integrin activation in more detail than for other integrins. To assess cellular function, we tested rolling and arrest in a microfluidic flow

chamber system and obtained high-resolution maps of the footprints of rolling and arrested cells by total internal reflection (TIRF) microscopy.

2 | MATERIALS AND METHODS

2.1 | Reagents

Alexa Fluor 488-conjugated β2 integrin conformation-specific antibody mAb24 to human β2-I-like-domain, which reports the headpiece opening,[21] PE-conjugated anti-CD18 mAb (IB4), and PE-conjugated anti-CXCR2 mAb (5E8) were purchased from Biolegends, San Diego, CA, USA. The KIM127 mAb to human β2-IEGFdomain, which reports the ectodomain extension,[22] was purified at the Lymphocyte Culture Center at the University of Virginia from hybridoma supernatant (American Type Culture Collection). KIM127 was directly labeled by DyLight 550 using DyLight antibody labeling kits from Thermo Fisher Scientific, Waltham, MA, USA. Monoclonal anti-actin (Millipore Sigma, St Louis, MO, USA, 1:5000), monoclonal anti-talin-1 (8d4, Millipore Sigma, St Louis, MO, USA, 1:1000) were used for immunoblotting. Recombinant human P-selectin-Fc, ICAM-1-Fc, and IL-8 were purchased from R&D Systems, Minneapolis, MN, USA. Casein blocking buffer was purchased from Thermo Fisher Scientific, Waltham, MA, USA. CellMask DeepRed and CellTracker Orange CMRA were purchased from Thermo Fisher Scientific, Waltham, MA, USA. RPMI 1640, with or without phenol red, and PBS without Ca^{2+} and Mg^{2+} were purchased from Thermo Fisher Gibco. HSA was purchased from Gemini Bio Products, West Sacramento, CA, USA.

2.2 | cDNAs and recombinant proteins

The cDNAs encoding the full-length human αL and β2 proteins were amplified by RT-PCR and cloned into a pLVX lentiviral expression vector. Cloning of β2 point mutants L697P was done by oligonucleotide-directed mutagenesis using Infusion-HD Eco Dry Cloning Kit (Takara Bio USA, Inc. Clontech, Mountain View, CA, USA). The pCas9-enhanced GFP (EGFP) plasmid was purchased from Addgene, Watertown, MA, USA (plasmid #48138). The pTLN1gRNA-Cas9-DasherGFP plasmid was provided by Horizon Discovery (Cambridge, United Kingdom). The sgRNA sequences were as followed: β2-sgRNA1: gccgggaatgcatcgagtcg *ggg*; β2-sgRNA2: gtgacgctttacctgcgacc *agg* (PAM sequences are highlighted by italic and underline). TLN1-gRNA: GGATCCGCTCACGAATGATG. All constructs were confirmed by DNA sequencing.

2.3 | Cell culture experiments

CXCR2-expressing HL-60 cells were a gift from Dr. Ann Richmond at the Vanderbilt University School of Medicine.[23] Cells were selected with G418 (0.5 μg/ml) to keep CXCR2 expression and routinely tested for mycoplasma infection. To make HL-60 β2 KO cells, HL-60 cells were co-transfected with β2-sgRNA1 and 2 and Cas9-EGFP using Amaxa electroporator (Lonza Group AG, Basel, Switzerland) followed by cell sorting of EGFP positive cells. Five to seven days later, the HL-60 β2 KO cells were incubated with anti-β2 antibody, and β2 null cells were sorted by flow cytometry (BD FACSAria II). The HL-60 β2-KO cells were reconstituted with β2-WT or β2-L697P by lentiviral transduction followed by selection with puromycin and FACS sorting for similar β2 expression. To generate the

HL-60-talin KO cells, HL-60 cells were transfected with pTLN1gRNA-Cas9-DasherGFP using Amaxa electroporator (Lonza Group AG, Basel, Switzerland) followed by cell sorting of EGFP positive cells. Single clones of TLN1-KO HL-60 cells were generated by limiting dilution in 96-well plates and confirmed by Western blotting using anti-talin antibodies (Millipore Sigma, St Louis, MO, USA).

2.4 | Microfluidic perfusion assay

The assembly of the multichannel microfluidic devices used in this study and the coating of coverslips with recombinant human P-selectin-Fc, ICAM-1-Fc, and IL-8 has been described previously.[3,12,19] Briefly, coverslips were coated with P-selectin-Fc (2 μg/ml), ICAM1-Fc (10 μg/ml), and IL-8 (5 μg/ml) for 2 h and then blocked for 1 h with casein (1%) at room temperature (RT). After coating, coverslips were sealed to polydimethylsiloxane chips by magnetic clamps to create flow chamber channels ~29 μm high and ~300 μm across. By modulating the pressure between the inlet well and the outlet reservoir, a wall shear stress of 2 or 6 dyn/cm^2 was applied. HL-60 cells (5×10^6 cells/ml) were perfused in the microfluidic device over a substrate of recombinant human P-selectin-Fc, recombinant human ICAM-1-Fc with or without IL-8. The rolling and arrest of cells were recorded by an IX71 inverted research microscope (Olympus America Inc, Cypress, CA, USA) with a 10× NA 0.3 air objective. The number of rolling and arrested cells were counted in 5 channels per group. The rolling duration and rolling distance were acquired from the images by analyzing 15 cells started rolling to arrest.

2.5 | Flow cytometry

To assess the expression of CD18 and CXCR2 on different HL-60 cell lines, 5×10^6 cells/ml HL60 cells were incubated with PE-conjugated anti-CD18 mAb (clone IB4, 10 μg/ml) or PE-conjugated anti-CXCR2 mAb (clone 5E8, 10 μg/ml) at RT for 10 min. The same staining of isotype antibodies was used as negative controls. Cell fluorescence was assessed with an LSRII (BD Biosciences, San Jose, CA) and was analyzed with FlowJo software (version 10.4).

To monitor the dynamics of β_2 integrin activation, 400 μL 2.5×10^5 cells·mL^{-1} HL60 cells were assessed by an LSRII analyzer (BD Biosciences, San Jose, CA) for 10 s. After adding 0.5 μg/ml AF488-conjugated mAb24 and DL550-conjugated KIM127 (final concentration), cells were put back to the analyzer for another 5 min. Then after adding 1 μg/ml IL-8, cells were put back to the analyzer for another 10 min. The curves showing the dynamics of integrin activation were generated by FlowJo software (version 10.4). The quantification of mAb24 and KIM127 MFI was analyzed by FlowJo software (version 10.4) and obtained from 5 individual experiments. Compensations were performed before all experiments.

2.6 | Immunoprecipitation and blotting

Cells were lysed with ice-cold cell lysis buffer (50 mM Tris-HCl, pH 7.4, 100 mM NaCl, 10 mM $MgCl_2$, 1%NP40, and 10% glycerol) plus protease inhibitor cocktails (Roche AG, Basel, Switzerland) on ice for 30 min and separated on a 4%–20% SDS-polyacrylamide gel (Novex; Invitrogen, Carlsbad, CA, USA). Western blots were stained with monoclonal anti-talin (8d4, Sigma, 1:1000) and monoclonal anti-actin (Sigma, 1:5000). Signal was detected

and results quantified using an Odyssey imaging system (LI-COR Biosciences, Lincoln, NE, USA).

2.7 | TIRF imaging

The TIRF setup and the theory of TIRF has been described previously in detail.[3,24] The setup consisted of an IX71 inverted TIRF research microscope (Olympus America Inc, Cypress, CA, USA) with a 100 × NA 1.45 plan-apochromatic oil immersion TIRF microscopy objective and 5 mW blue (λ = 488 nm), 5 mW yellow-green (λ = 561 nm), and 2 mW red (λ = 641 nm) diode-pumped solid-state lasers (CVI Melles Griot) as TIRF excitation light sources. Images were captured at a rate of one frame per second using a QV2 (Photometrics) QuadView video coupler and a 16-bit digital charge-coupled device camera (Hamamatsu C10600–10B ORCA-R2). The laser shutters and camera were controlled with the SlideBook 5.5 software (Intelligent Imaging Innovations). The absorption and emission peaks of the fluorochromes used in this study were, respectively, 493 and 518 nm for DL488, 562 and 576 nm for DL550, and 649 and 666 nm for CellMask DeepRed. There was no bleed-through between channels. A TIRF incidence angle of θ = 70° was used for all 3 lasers in all TIRF experiments.

The homogeneous binding assay (the continuous real-time measurement without separation of soluble antibody) and TIRF imaging were combined as described previously.[3] Briefly, during the assay, HL60 cells (2.5×10^6 cells/ml) were incubated with AF488-conjugated mAb24 and DL550-conjugated KIM127 (5 μg/ml each) for 3 min at RT and immediately perfused through the microfluidic device at a wall shear stress of 6 dyn/cm^2 without separation of the soluble mAbs. The plasma membrane of neutrophils was labeled with CellMask DeepRed according to the manufacturer's instructions (10^6 cells/ml, 1μM, RT 10 min, followed by 2 washes with PBS) before incubation with mAbs. When neutrophils were observed rolling on the substrate, the acquisition was started using TIRF microscopy to acquire the dynamics of integrin activation on neutrophil footprints during rolling (~10 s), arrest and ~10–200 s following arrest.

To assess the Mn^{2+}-induced cell spreading, the 8-well μ-Slide chamber with a glass bottom (ibidi) was coated with 5 μg/ml recombinant human ICAM-1-Fc at 37°C for 30 min. A total of 2×10^6 cells/ml HL-60 cells were labeled with 4μM CellTracker Orange CMRA at RT for 1 h. After 2 washes with PBS, cells were re-suspended in PBS plus 1μM Mn^{2+} and placed into the coated chambers for 5 min. After the fixation with 1% PFA for 5 min and 2 washes with PBS, cells were imaged by epifluorescence and TIRF microscopy.

2.8 | Statistical analysis

Statistical analysis was performed in PRISM software (version 6.00, GraphPad Software), and all datasets were checked for Gaussian normality distribution. Data analysis was performed using 1-way ANOVA or 2-way ANOVA with Bonferroni posttest, which is indicated in figure legends. The resulting P values are indicated as follows: n.s.: not significant, $P > 0.05$; *, $0.01 < P < 0.05$; **, $0.001 < P < 0.01$; ***, $P < 0.001$. Data represent the mean ± SD or SEM of at least 3 independent experiments. Western blot results are shown as representative images from at least 3 independent experiments.

3 | RESULTS

3.1 | Blocking the transmission of β2 TMD topology impairs chemokine-induced β2 integrin-dependent arrest of rolling leukocytes

Alignment of the human β3 and β2 TMDs shows that Leu^{697} in β2 is equivalent to Ala^{711} in β3, which was mutated to Pro in β3[20,25] (Fig. 1A, top panel). A 3D model of the TMD of the integrin β2 subunit, based on integrin β3, shows that the proline mutation breaks a critical hydrogen bond in the transmembrane helix and introduces a flexible kink (Fig. 1A, bottom panel). To test the effect of the β2-L697P mutation, we first knocked out (KO) the *ITGB2* gene that encodes β2 by CRISPR/Cas9 mutagenesis[23] in HL-60 cells stably transfected with the chemokine receptor CXCR2,[26] resulting in complete loss of β2 surface expression (Fig. 1B, top, second panel). These β2-KO HL-60 cells (negative control) were transfected with wild-type β2 (WT, positive control, third panel) or β2-L697P (test case, fourth panel). As a second negative control, we knocked out *TLN1* encoding talin-1. Surface expression of β2 (CD18) assessed by mAb M18/2 (conformation-independent) was comparable in all cell lines (Fig. 1B). CXCR2 expression was comparable among the four reconstituted cell lines (Fig. 1B). Talin-1 knockout was confirmed by Western blot (Fig. 1C).

The manipulated cells were perfused in a previously described P-selectin and ICAM-1-coated microfluidic system[3] at 6 dyn/cm^2. Under baseline conditions, most HL-60 cells rolled. Adding IL-8 to the substrate coating significantly increased the number of arrested cells. This increase in arrest was completely absent in β2-KO HL-60 cells (Fig. 2A) and in cells reconstituted with β2-L697P (Fig. 2A), suggesting that the arrest function was completely dependent on transmission through a stiff TMD. Cell rolling and arrest was also tested at a wall shear stress of 2 dynes/cm^2 (Fig. 2C).

HL-60 β2-KO cells reconstituted with WT β2 rolled at a median velocity of ~ 2.1 μm/s (Fig. 2B), which is much lower than the velocity of β2 knockout HL-60 cells (6.5 μm/s). This indicates that some of the β2 integrins are in the E$^+$ conformation even under control conditions. This rolling velocity was significantly ($P < 0.0001$) reduced to ~0.1 μm/s when IL-8 was added, suggesting that more E$^+$ integrins were available. HL-60 β2-KO cells reconstituted with β2-L697P rolled at a median velocity of ~5.5 μm/s, which is significantly ($P = 0.0020$) higher than cells reconstituted with WT β2. Most importantly, this velocity did not change when IL-8 was added, suggesting that the extracellular domain was unable to extend when the proline L697P mutation prevented transmission of the conformational change.

3.2 | Blocking the transmission of β2 TMD topology impaired chemokine-induced extension but not high affinity of β2 integrins

The flow-cytometry-based homogenous binding assay was used to report the dynamic changes of integrin conformations.[3,27] In the same assay, the β2 extension was induced by exposure to IL-8 as reported by KIM127 reactivity (Fig. 3A). The KIM127 signal was reduced in HL-60 β2-KO cells reconstituted with β2-L697P. Statistical analysis showed that this defect was significant (Fig. 3B). Unreconstituted β2-KO HL-60 cells and talin-1 deficient HL-60 cells served as negative controls. Thus, based on the β2 conformation

reporter antibodies, the L697P mutation partially reduces extension and slightly affects high affinity, whereas talin-1 KO cells have almost complete defects in both extension and high affinity. HL-60 cells reconstituted with the TMD kink mutant have a less severe defect than talin-1 knockout cells.

Flow cytometry showed that IL-8 induces the high-affinity conformation of β2 integrin in HL-60 β2-KO cells reconstituted with WT β2 as reported by mAb24 binding (Fig. 3A). Unreconstituted HL-60 β2-KO cells served as a negative control. The same increase in mAb24 MFI as in WT β2 was observed in cells reconstituted with β2-L697P. Statistical analysis showed that there was a slight decrease in the induction of mAb24 MFI, but there was no significant difference in the signal between HL-60 cells reconstituted with wild-type β2 or β2-L697P. This suggests that β2-L697P is still able to transmit most of the conformational change necessary for high affinity (Fig. 2B). The talin-1 KO HL-60 cells served as a negative control and showed a complete inability of inducing mAb24 reactivity after exposure to IL-8. Thus, the TMD kink does not show a significant defect in inducing the mAb24 epitope.

3.3 | Blocking the transmission of β2 TMD topology impaired chemokine-induced β2 integrin activation, adhesion and spreading of cells by inside-out but not outside-in signaling

After arrest, adherent neutrophils and HL-60 cells spread on suitable substrates. We tested this by perfusing cells on P-selectin, ICAM-1, and IL-8 by using quantitative dynamic footprinting microscopy.[3,24,28] Under these conditions, many integrin molecules are engaged after IL-8 stimulation. In this setting, both integrin inside-out and outside-in signaling[29] contribute to the phenotype because less integrin activation induced by IL-8 (inside-out) will lead to fewer activated integrin molecules and thus reduced outside-in signaling. HL-60 β2-KO cells reconstituted with WT β2 showed extensive spreading (Fig. 4A). By contrast, HL-60 β2-KO cells reconstituted with β2-L697P showed reduced spreading, resulting in a much smaller footprint as observed by TIRF microscopy (Fig. 4A). The number and the mean area of clusters of activated integrins (both KIM127 and mAb24) were reduced in cells reconstituted with β2-L697P compared to those in the footprint of a cell reconstituted with WT β2 (Fig. 4B–C).

To test whether the defect of cell spreading and integrin activation in cells reconstituted with β2-L697P is caused by the impairment of integrin inside-out or outside-in signaling, we used the extracellular integrin activator, Mn^{2+}, to bypass the need for inside-out signaling (Fig. 5A, B). Mn^{2+}-treated HL-60 β2-KO cells reconstituted with WT β2 or β2-L697P showed extensive spreading, similar to unmanipulated HL-60 cells. This was evident in the size of the cell projection (Fig. 5B, left panel) and the size of the footprint, i.e., the area of the cell in close contact with the substrate (right panel). These findings suggest that the L697P mutation does not affect the outside-in signaling of HL-60 cells. The negative controls HL-60 β2-KO and HL-60 talin-1 KO did not spread and stayed round (Fig. 5A–B). Taken together, inhibition of topology changes of β2 TMD affects integrin activation, cell adhesion, and spreading by impairing inside-out but not outside-in signaling.

4 | DISCUSSION

Here, we show that introducing a TMD kink into β2 integrin completely blocks cell arrest under flow, largely by preventing β2 integrin extension. The defect is similar to but less complete than the defect seen in talin-1 knockout cells. We did not observe an impact of the TMD kink on the high-affinity (H^+) conformation.

"Inside-out signaling" is the capacity of intracellular signals mediated through the integrin cytoplasmic domains to regulate the affinity and function of integrin extracellular domains.[30] The prevailing model, mostly based on studies with platelet integrin αIIbβ3, proposes that talin, by binding to the β3 integrin cytoplasmic domain, disrupts an electrostatic interaction that stabilizes the inner membrane clasp that promotes the αIIbβ3 TMD association and changes the topology of β TMD, thereby disrupting an outer membrane clasp to complete the activation process.[25] A similar study proved the significance of transmission of β7 subunit TMD topology across the membrane.[19] However, neither αIIbβ3 nor α4β7 integrins contain I domains in their α chains. It is likely that the activation of I domain-containing integrins differs from that of integrins without I domain. Indeed, recent studies have indicated marked differences in the mechanisms of inside-out activation of other classes of integrins.[31] In this study, we provide evidence that transmitting conformation changes across the plasma membrane is important for the functionality of β2 integrins, the first study of integrins with I domains. The second major finding is that TMD transmission appears to be important for integrin extension only and not for high affinity. As expected, talin-1-deficient cells showed a nearly complete defect in both extension and high affinity. Thus, our findings support a model in which talin-1 binding to the β2 cytoplasmic tail has at least 2 functions, one of which is affected by the proline mutation L697P and the other is not.

During integrin inside-out activation, rearrangements in the αI domain coupled with a series of global and local conformational changes result in high affinity for ligand. For β2 integrins, this affinity increase has been reported to be by 10,000-fold.[32] The "switchblade" model of integrin activation[3,33] suggests a 2-step activation process in which integrin extension (E^+) is followed by a rearrangement in the ligand-binding site leading to high-affinity (H^+). In this study, we found that the β2 proline mutation partially reduces extension (E^+) but has no effect on high affinity (H^+). However, talin-1 KO cells have almost complete defects in both extension and high-affinity states. The binding of talin is important for the β2 integrin high-affinity state as shown by the inability of talin knockout cells to bind mAb24. However, this is not dependent on a stiff TMD, because the β2 TMD kink mutant has no defect in inducing the H^+ conformation. In the β2 kink mutant cells, most of the mAb24 reactivity likely resides in high-affinity bent integrin molecules, which cannot mediate binding in trans and therefore cannot mediate arrest.[3,12] The transmission of the talin-induced β2 tilt angle change also plays a critical role in β2 integrin extension. This is consistent with,[34] who showed that talin-1 W359A fails to support arrest and slow rolling. In the same study, another talin-1 mutant, L325R, also failed to support arrest, but was still able to support slow rolling. Thus, talin L325R is able to produce at least some β2 tilt angle change. Our data suggest that preventing the tilt angle change to be transmitted across the plasma membrane by introducing the β2 L697P kink does not allow sufficient integrin extension to support slow rolling.

We recently showed that β2 integrins could assume a high-affinity bent (E^-H^+) conformation that interacts with ICAMs in cis (on the same cell).[3] This cis interaction effectively inhibits cell adhesion as evidenced by prolonged rolling distance, prolonged rolling time, and reduced number of adherent neutrophils, thereby providing an autoinhibitory mechanism that suppresses inflammatory responses. The cis interaction of β2 integrins with other ligands, such as FcγRIIA, was demonstrated by an independent study.[35] Based on our findings by flow cytometry, microscopy, and cell function (arrest, slow rolling, spreading), we conclude that the E^-H^+ conformation is not affected by introducing the β2 TMD kink.

Interestingly, the defect in β2 extension in TMD kink cells as reported by KIM127 binding in flow cytometry was incomplete, but the arrest defect and the slow rolling defect were nearly complete. Most likely, this reflects the ability of KIM127 to bind partially extended β2.[36] Indeed, β2 integrins are known to "breathe," which means thermodynamically driven slight extension that reverts to the bent conformation.[37,38] KIM127 can bind as soon as the "knee" of β2 is even slightly unbent.[22] In the flow cytometry assay, such slightly unbent β2 can bind KIM127, but this slightly unbent conformation is not sufficient to mediate arrest or slow rolling. Thus, we conclude that the TMD kink mutant still allows "breathing" of β2 integrins, but not true, full extension, which is needed to bind ligand in trans as required for arrest from flow (E^+H^+) and slow rolling (E^+H^-).

Integrin outside-in activation is required for postarrest events like the spreading of cells onto the substrate. Our data show that β2-L697P cells possess reduced cell spreading ability and much smaller footprints as assessed by TIRF microscopy (Fig. 4A). Thus, blocking transmission of the talin-induced change in β2 TMD topology disrupts integrin β2 mediated cell spreading. However, the spreading defect could be overcome by adding the exogenous activator Mn^{2+}, which allowed cells reconstituted with the β2 TMD kink mutant to spread fully. The capacity of Mn^{2+} to stimulate β2-L697P cells spreading on ICAM-1 indicates that this mutation did not disrupt the ability of the integrin to transmit outside-in signals. Thus, it follows that outside-in signaling is not mediated by the rigidity of the β2 TMD. We previously made similar observations in β7 TMD kink mutants.[19]

Our data show that the β2L697P mutation inhibits integrin activation and cell adhesion under flow, suggesting that the strength of the β2L697P bonds with ICAM-1 bonds is decreased. β2 integrins have previously been shown to be catch bonds,[39,40] whose lifetime increases with applied force. We show that the L697P mutation affects the conformation of the extracellular domain of β2, which may also affect its catch bond behavior.

In conclusion, introducing a flexible kink in the TND or β2 integrin leads to a complete defect in cell arrest, slow rolling, and initial spreading. Based on the reporter antibody binding, the high-affinity (H^+) conformation is unaffected, which is different from talin-1 knockout cells, where both extension and high affinity are defective. Based on KIM127 binding, the β2 TMD kink still allows partial unbending of the β2 knee, but not true, full extension, which is needed for slow rolling (E^+H^-) and arrest (E^+H^+). This partial defect in β2 integrin activation reveals that the conformation change transmitted by the rigid TMD is not the only conformation change induced by talin-1 binding.

ACKNOWLEDGMENTS

This work was supported by grants from the National Institutes of Health, USA (HL078784 to M.H.G. and K.L., R01HL145454 to Z.F.) and WSA postdoctoral fellowships (17POST33660181 to H.S., 16POST31160014 to Z.F.) and the Career Development Award (18CDA34110426 to Z.F.) from the American Heart Association, USA.

Abbreviations

Cas9	CRISPR associated protein 9
E^+	extended conformation
H^+	high affinity conformation
HSA	human serum albumin
ICAM-1	intercellular adhesion molecule 1
IL-8	interleukin-8
KO	knockout
MFI	mean fluorescence intensity
PAM	protospacer adjacent motif
PBS	phosphate-buffered saline
PE	phycoerythrin
PSGL-1	P-selectin glycoprotein ligand-1
RT	room temperature
sgRNA	single guide RNA
Syk	spleen tyrosine kinase
TIRF	total internal reflection fluorescence
TMD	transmembrane domain
WT	wild type

REFERENCES

1. Diacovo TG, Roth SJ, Buccola JM, Bainton DF, Springer TA. Neutrophil rolling, arrest, and transmigration across activated, surface-adherent platelets via sequential action of P-selectin and the beta 2-integrin CD11b/CD18. Blood. 1996;88(1):146–157. [PubMed: 8704169]
2. Fan Z, Ley K. Leukocyte arrest: biomechanics and molecular mechanisms of beta2 integrin activation. Biorheology. 2015.
3. Fan Z, McArdle S, Marki A, et al. Neutrophil recruitment limited by high-affinity bent beta2 integrin binding ligand in cis. Nat Commun. 2016;7:12658. [PubMed: 27578049]
4. Yago T, Zhang N, Zhao L, Abrams CS, McEver RP. Selectins and chemokines use shared and distinct signals to activate beta2 integrins in neutrophils. Blood Adv. 2018;2(7):731–744. [PubMed: 29592875]

5. Fan Z, Ley K. Leukocyte arrest: biomechanics and molecular mechanisms of beta2 integrin activation. Biorheology. 2015;52(5–6): 353–377. [PubMed: 26684674]
6. Zarbock A, Ley K, McEver RP, Hidalgo A. Leukocyte ligands for endothelial selectins: specialized glycoconjugates that mediate rolling and signaling under flow. Blood. 2011;118:6743–6751. [PubMed: 22021370]
7. Zarbock A, Ley K. Neutrophil adhesion and activation under flow. Microcirculation. 2009;16:31–42. [PubMed: 19037827]
8. Kuwano Y, Spelten O, Zhang H, Ley K, Zarbock A. Rolling on E- or P-selectin induces the extended but not high-affinity conformation of LFA-1 in neutrophils. Blood. 2010;116(4):617–624. [PubMed: 20445017]
9. Morikis VA, Chase S, Wun T, Chaikof EL, Magnani JL, Simon SI. Selectin catch-bonds mechanotransduce integrin activation and neutrophil arrest on inflamed endothelium under shear flow. Blood. 2017;130(19):2101–2110. [PubMed: 28811304]
10. Robinson MK, Andrew D, Rosen H, et al. Antibody against the Leu-CAM β-chain (CD18) promotes both LFA-1-dependent and CR3-dependent adhesion events. J Immunol. 1992;148:1080–1085.s [PubMed: 1371129]
11. Dransfield I, Hogg JC. Regulated expression of Mg^{2+} binding epitope on leukocyte integrin α subunits. EMBO J. 1989;8:3759. [PubMed: 2479549]
12. Fan Z, Kiosses WB, Sun H, et al. High-affinity bent beta2-integrin molecules in arresting neutrophils face each other through binding to ICAMs in cis. Cell Rep. 2019;26(1):119–130 e115. [PubMed: 30605669]
13. Moser M, Legate KR, Zent R, Fassler R. The tail of integrins, talin, and kindlins. Science. 2009;324(5929):895–899. [PubMed: 19443776]
14. Lefort CT, Rossaint J, Moser M, et al. Distinct roles for talin-1 and kindlin-3 in LFA-1 extension and affinity regulation. Blood. 2012;119:4275–4283. [PubMed: 22431571]
15. Shattil SJ, Kim C, Ginsberg MH. The final steps of integrin activation: the end game. Nat Rev Mol Cell Biol. 2010;11(4):288–300. [PubMed: 20308986]
16. Tadokoro S, Shattil SJ, Eto K, et al. Talin binding to integrin beta tails: a final common step in integrin activation. Science. 2003;302(5642): 103–106. [PubMed: 14526080]
17. Lau TL, Kim C, Ginsberg MH, Ulmer TS. The structure of the integrin alphaIIbbeta3 transmembrane complex explains integrin transmembrane signalling. EMBO J. 2009;28:1351–1361. [PubMed: 19279667]
18. Kim C, Lau TL, Ulmer TS, Ginsberg MH. Interactions of platelet integrin alphaIIb and beta3 transmembrane domains in mammalian cell membranes and their role in integrin activation. Blood. 2009;113:4747–4753. [PubMed: 19218549]
19. Sun H, Lagarrigue F, Gingras AR, Fan Z, Ley K, Ginsberg MH. Transmission of integrin beta7 transmembrane domain topology enables gut lymphoid tissue development. J Cell Biol. 2018.
20. Kim C, Ye F, Hu X, Ginsberg MH. Talin activates integrins by altering the topology of the beta transmembrane domain. J Cell Biol. 2012;197(5):605–611. [PubMed: 22641344]
21. Lu C, Shimaoka M, Zang Q, Takagi J, Springer TA. Locking in alternate conformations of the integrin alphaLbeta2I domain with disulfide bonds reveals functional relationships among integrin domains. Proc Natl Acad Sci U S A. 2001;98(5):2393–2398. [PubMed: 11226250]
22. Lu C, Ferzly M, Takagi J, Springer TA. Epitope mapping of antibodies to the C-terminal region of the integrin beta 2 subunit reveals regions that become exposed upon receptor activation. J Immunol. 2001;166(9):5629–5637. [PubMed: 11313403]
23. Ran FA, Hsu PD, Wright J, Agarwala V, Scott DA, Zhang F. Genome engineering using the CRISPR-Cas9 system. Nat Protoc. 2013;8(11):2281–2308. [PubMed: 24157548]
24. Sundd P, Gutierrez E, Pospieszalska MK, Zhang H, Groisman A, Ley K. Quantitative dynamic footprinting microscopy reveals mechanisms of neutrophil rolling. Nat Methods. 2010;7(10):821–824. [PubMed: 20871617]
25. Kim C, Schmidt T, Cho EG, Ye F, Ulmer TS, Ginsberg MH. Basic amino-acid side chains regulate transmembrane integrin signalling. Nature. 2012;481(7380):209–213.

26. Sai J, Walker G, Wikswo J, Richmond A. The IL sequence in the LLKIL motif in CXCR2 is required for full ligand-induced activation of Erk, Akt, and chemotaxis in HL60 cells. J Biol Chem. 2006;281(47):35931–35941. [PubMed: 16990258]
27. Chigaev A, Blenc AM, Braaten JV, et al. Real time analysis of the affinity regulation of alpha 4-integrin. The physiologically activated receptor is intermediate in affinity between resting and Mn(2+) or antibody activation. J Biol Chem. 2001;276(52):48670–48678. [PubMed: 11641394]
28. Sundd P, Gutierrez E, Koltsova EK, et al. 'Slings' enable neutrophil rolling at high shear. Nature. 2012;488(7411):399–403. [PubMed: 22763437]
29. Abram CL, Lowell CA. The ins and outs of leukocyte integrin signaling. Annu Rev Immunol. 2009;27:339–362. [PubMed: 19302044]
30. Ginsberg MH, O'Toole TE, Loftus JC, Plow EF. Ligand binding to integrins: dynamic regulation and common mechanisms. Cold Spring Harb Symp Quant Biol. 1992;57:221–231. [PubMed: 1339661]
31. Lu Z, Mathew S, Chen J, et al. Implications of the differing roles of the beta1 and beta3 transmembrane and cytoplasmic domains for integrin function. Elife. 2016;5.
32. Shimaoka M, Takagi J, Springer TA. Conformational regulation of integrin structure and function. Annu Rev Biophys Biomol Struct. 2002;31:485–516. [PubMed: 11988479]
33. Luo BH, Carman CV, Springer TA. Structural basis of integrin regulation and signaling. Annu Rev Immunol. 2007;25:619–647. [PubMed: 17201681]
34. Yago T, Petrich BG, Zhang N, et al. Blocking neutrophil integrin activation prevents ischemia-reperfusion injury. J Exp Med. 2015;212(8):1267–1281. [PubMed: 26169939]
35. Saggu G, Okubo K, Chen Y, et al. Cis interaction between sialylated FcgammaRIIA and the alphaI-domain of Mac-1 limits antibody-mediated neutrophil recruitment. Nat Commun. 2018;9(1):5058. [PubMed: 30498196]
36. Schurpf T, Springer TA. Regulation of integrin affinity on cell surfaces. Embo J. 2011;30(23): 4712–4727. [PubMed: 21946563]
37. Takagi J, Petre BM, Walz T, Springer TA. Global conformational rearrangements in integrin extracellular domains in outside-in and inside-out signaling. Cell. 2002;110(5):599–511. [PubMed: 12230977]
38. Askari JA, Buckley PA, Mould AP, Humphries MJ. Linking integrin conformation to function. J Cell Sci. 2009;122(Pt 2):165–170. [PubMed: 19118208]
39. Chen W, Lou J, Evans EA, Zhu C. Observing force-regulated conformational changes and ligand dissociation from a single integrin on cells. J Cell Biol. 2012;199(3):497–512. [PubMed: 23109670]
40. Chen W, Lou J, Zhu C. Forcing switch from short- to intermediate- and long-lived states of the alphaA domain generates LFA-1/ICAM-1 catch bonds. J Biol Chem. 2010;285(46):35967–35978. [PubMed: 20819952]

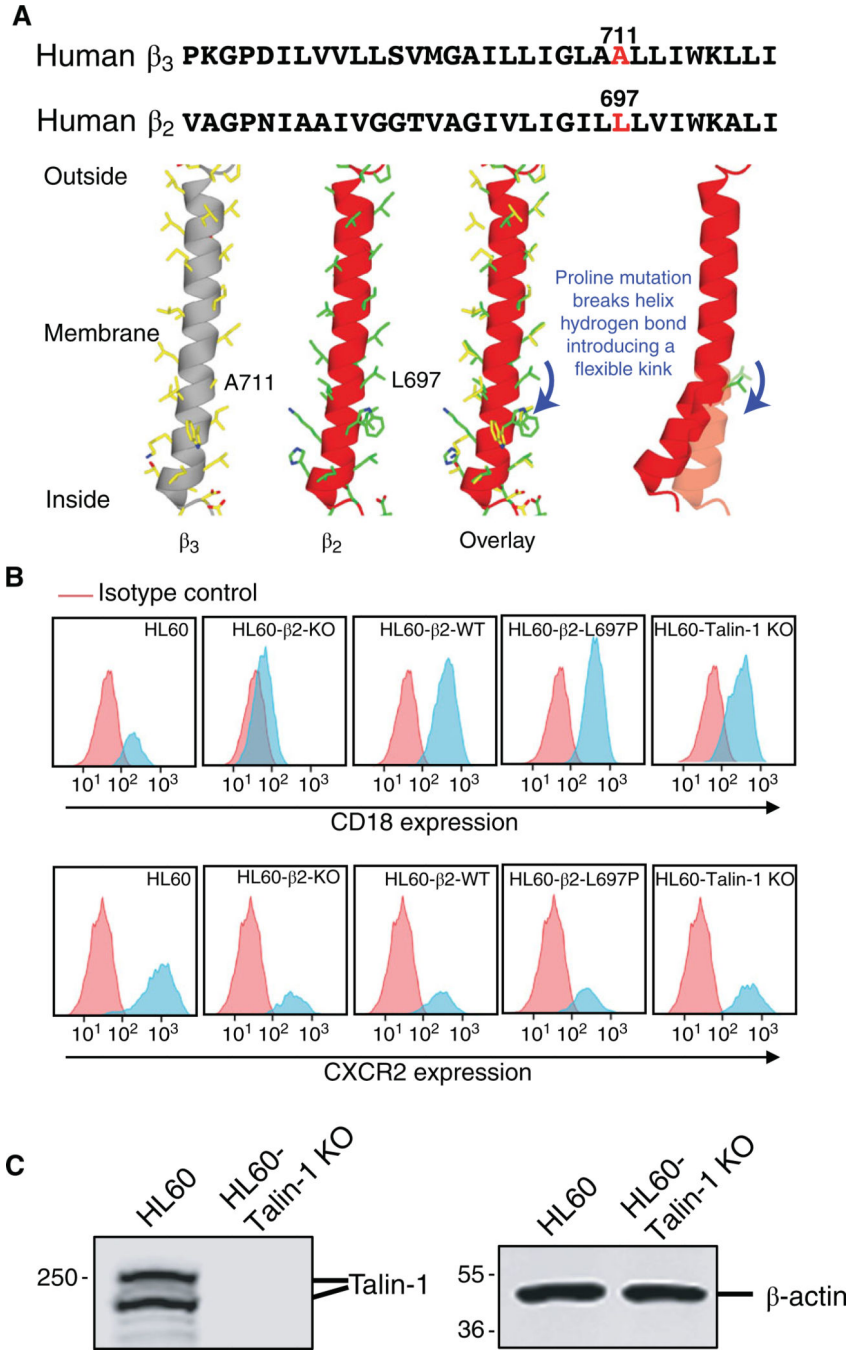

FIGURE 1. Generation of HL-60-*β*2 proline mutant cells and HL-60-talin-1 KO cells.

(**A**) Comparison of transmembrane domains (TMD) of human integrin *β*3 and *β*2 subunits. Sequence alignment in top panel. Proline mutant sites Ala^{711} in *β*3 and paralogous Leu^{697} in *β*2 highlighted in red. Bottom panel: 3D model of TMD of integrin *β*2 (red) compared to integrin *β*3 (grey). (**B**) *β*2 (CD18, top) and CXCR2 (bottom) expression on the surface of CXCR2-transfected HL-60 cells (HL60), these same HL-60 in which *β*2 integrin was knocked out (HL60-*β*2-KO), reconstituted with wild-type *β*2 (HL60-*β*2-WT) or with the kink mutant (HL60-*β*2-L697P), compared to talin-1 knockout HL-60 cells (HL60-talin-1

KO) cells. (**C**) Expression of talin-1 in parental or talin-KO HL-60 cells. β actin as loading control

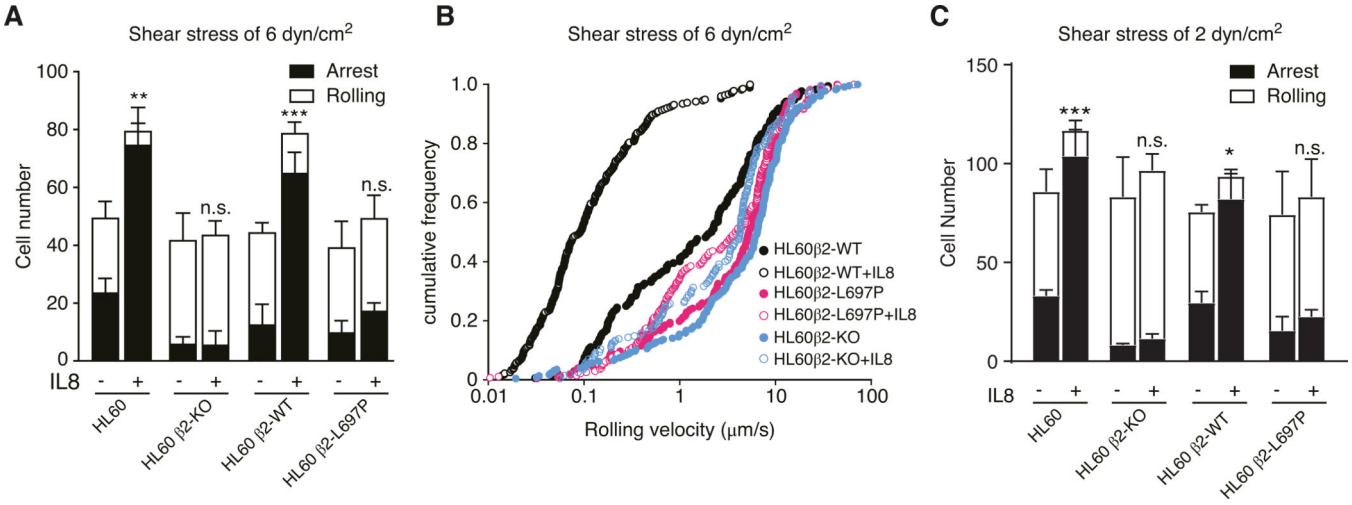

FIGURE 2. Blocking β2 TMD transmission of conformation change in response to IL-8 impairs chemokine-induced β2 integrin-dependent arrest of rolling leukocytes.

(**A**) Adhesive behavior of CXCR2-transfected differentiated HL-60 cells (HL60), HL60β2-KO cells, same cells reconstituted with β2 WT or β2-L697P on a substrate of P-Selectin/ICAM-1 with (+) or without (−) IL8 stimulation at a wall shear stress of 6 dyn/cm^2. Cells were pre-differentiated with 1.3% DMSO for 5–7 d and then infused into the flow chamber. (**B**) cumulative rolling velocity histograms for these same cells at 6 dyn/cm^2. (**C**) Like panel A, but at a wall shear stress of 2 dyn/cm^2. The arrested cell number (black, mean ±SD, $n = 5$ each in **A** and **C**) were analyzed. *$P < 0.05$, **$P < 0.01$, ***$P < 0.001$, n.s. $P > 0.05$ by 2-way ANOVA followed by Bonferroni posttest

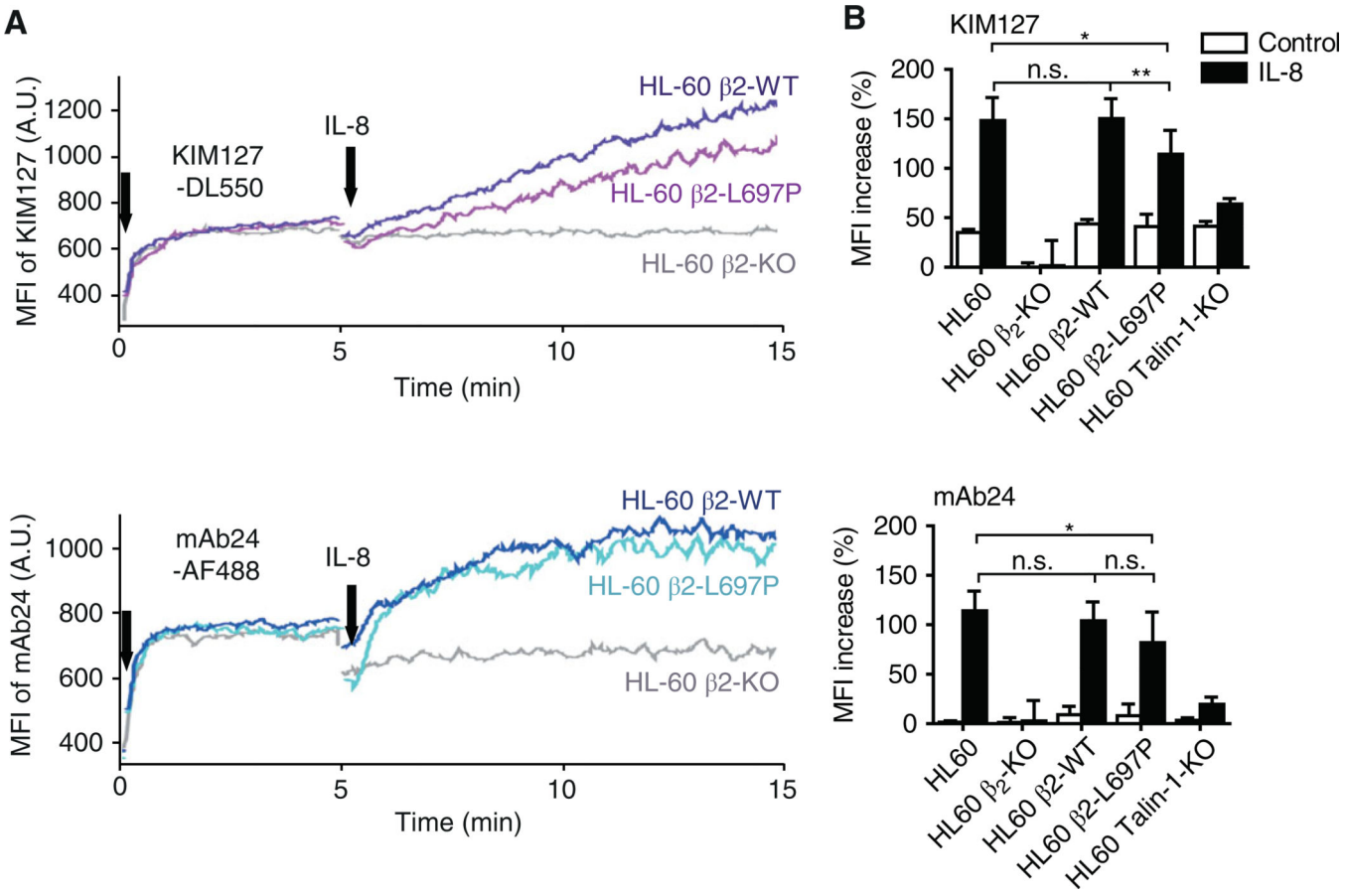

FIGURE 3. Blocking β2 TMD transmission of conformation change in response to IL-8 impairs chemokine-induced binding of extracellular β2 conformation reporter antibodies.

(**A**) Typical graphs showing dynamic expression of mAb24 (lower panel, high-affinity β2 integrins) and KIM127 (upper panel, extended β2 integrins) epitopes on β2-KO HL-60 cells reconstituted with β2-L697P (cyan or magenta curves in lower or upper panels, respectively), β2-WT (blue or purple curves in lower or upper panels, respectively), or unreconstituted CXCR2-transfected HL-60 cells (gray curves) in response to IL8 stimulation. Cells were differentiated with 1.3% DMSO for 5–7 d prior to the assay. (**B**) Bar graphs showing the mean fluorescence intensity (MFI) increase of mAb24 (lower panel) or KIM127 (upper panel) signal 10 min after IL8 stimulation. Mean ±SD, $n = 5$ individual experiments. *$P \leq 0.05$, **$P \leq 0.01$, n.s. $P > 0.05$ by 2-way ANOVA followed by Bonferroni posttest

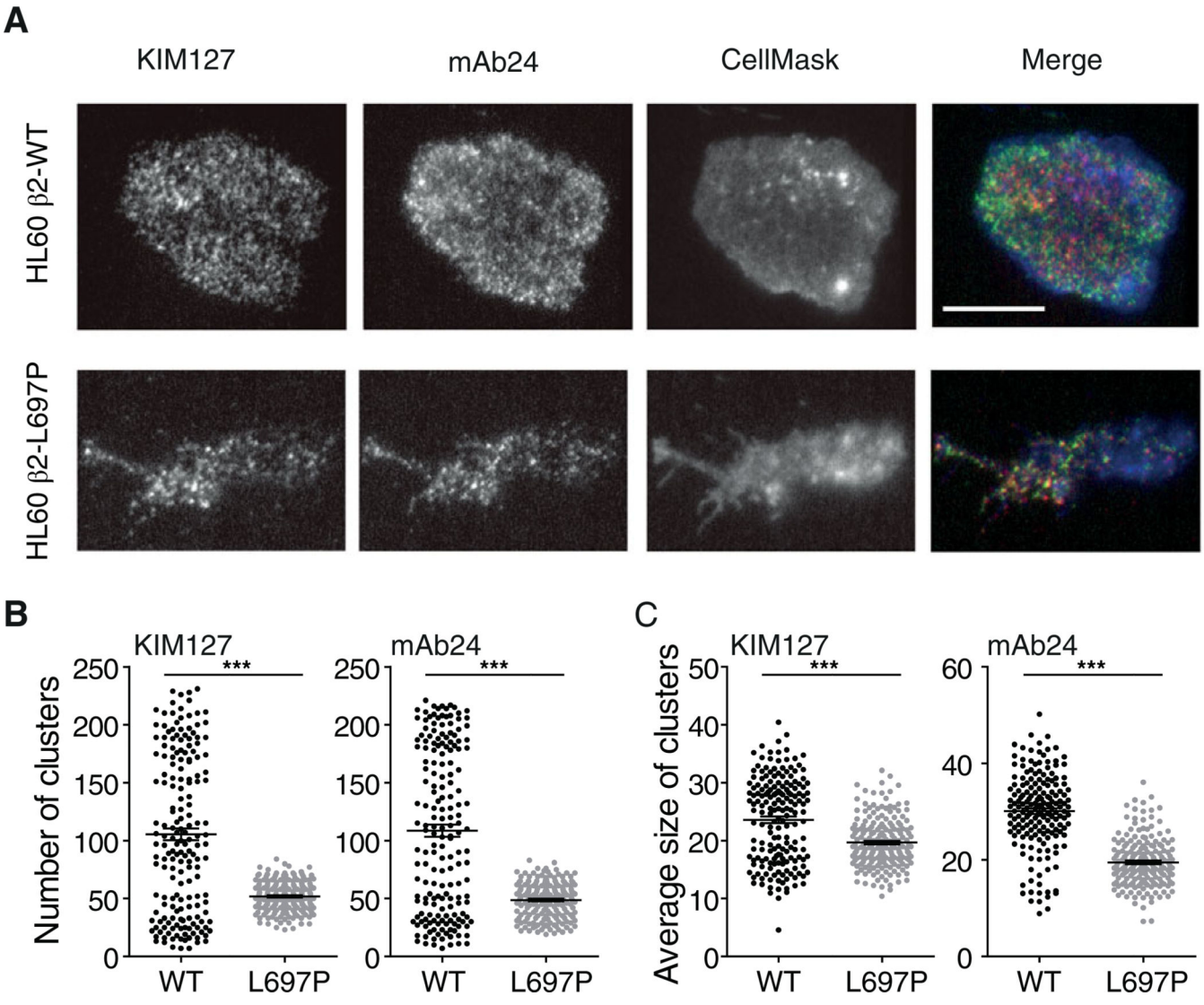

FIGURE 4. Blocking *β*2 TMD transmission of conformation change in *β*2 impairs integrin activation during leukocyte adhesion.

(**A**-**C**) 3 × 10^6/ml *β*2-KO CXCR2-transfected HL-60 cells reconstituted with *β*2-WT (top panel) or *β*2-L697P (bottom panel) were labeled with 1μM CellMask Deep Red (blue, membrane) at RT for 10 min, incubated with 5 μg/ml mAb24-AF488 (green, high-affinity *β*2 integrins) and KIM127-DL550 (red, extended *β*2 integrins) antibodies for 3 min, and perfused in the flow chamber coated with 2 μg/ml P-selectin, 10 μg/ml ICAM-1, and 5 μg/ml IL-8. Free antibodies remained present during the assay. Typical images of *β*2-L697P and WT cells 180 s after arrest (**A**). The total number of clusters (**B**) and the average cluster area (**C**) were analyzed. ***$P < 0.001$ in the 2-tail Student's *t*-test. Cells were differentiated with 1.3% DMSO for 5 d prior to the assay. Scale bar 10μm

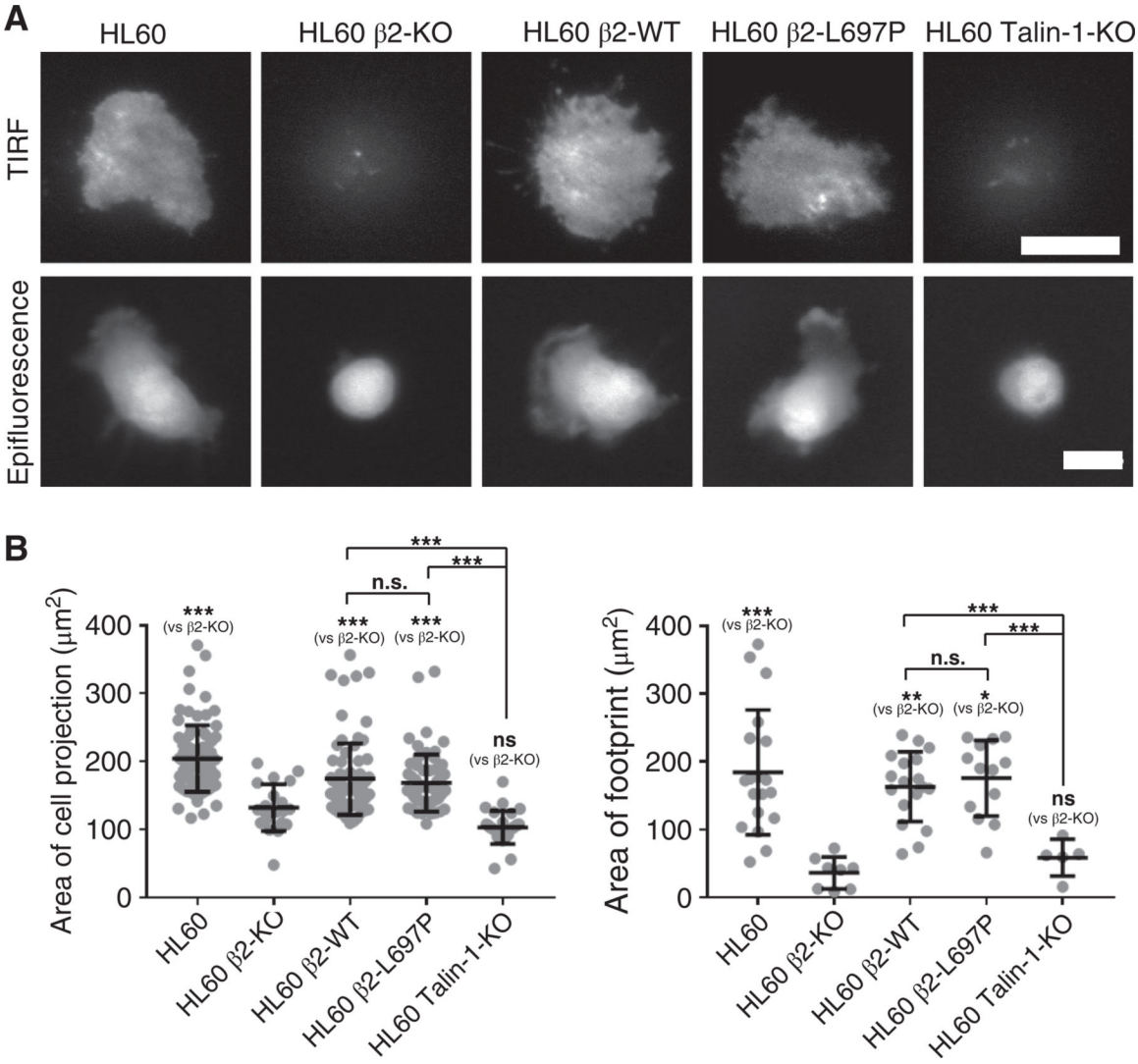

FIGURE 5. Blocking *β*2 TMD transmission of conformation change in *β*2 does not inhibit leukocyte spreading induced by *β*2 integrin outside-in signaling.

Mn^{2+} was used to force the activation of *β*2 integrin on cells. (**A**) Typical TIRF and epifluorescence images showed the footprints and cell bodies, respectively. WT CXCR2-transfected HL-60 cells (HL60), HL60 *β*2-KO cells reconstituted with *β*2-WT or *β*2L697P, compared with talin-1 KO HL60 cells on a substrate coated with 5μg/ml ICAM-1 (37°C, 30 min). Cells were differentiated with 1.3% DMSO for 5 d prior to the assay. Cells were labeled with 4 μM CMRA at RT for 1 h prior to the assay. Scale bars 10μm. (**B**) The area of cell projections (epifluorescence imaging) and footprints (TIRF imaging) was quantified for indicated cells. Mean ± SD. n = 81, 21, 79, 62, 28 for the cell projections of WT, *β*2-KO, *β*2-WT, *β*2-L697P, Tln1KO HL60 cells, respectively. n = 19, 8, 18, 13, 5 for the cell footprints of WT, *β*2-KO, *β*2-WT, *β*2-L697P, talin-1-KO HL60 cells, respectively. *P < 0.05, **P < 0.01, ***P < 0.001, n.s. P > 0.05 by one-way ANOVA followed by Bonferroni posttest